PHYSICAL REVIEW C **93**, 042501(R) (2016)

β-decay study within multireference density functional theory and beyond

M. Konieczka,[1] P. Bączyk,[1] and W. Satuła[1,2]
[1]*Faculty of Physics, University of Warsaw, ul. Pasteura 5, PL-02-093 Warsaw, Poland*
[2]*Helsinki Institute of Physics, P.O. Box 64, FI-00014 University of Helsinki, Finland*
(Received 16 September 2015; published 5 April 2016)

A pioneering study of Gamow-Teller (GT) and Fermi matrix elements (MEs) using no-core-configuration-interaction formalism rooted in multireference density functional theory is presented. After a successful test performed for ^{6}He $\rightarrow$ ^{6}Li β decay, the model is applied to compute MEs in the sd- and pf-shell $T = 1/2$ mirror nuclei. The calculated GT MEs and the isospin-symmetry-breaking corrections to the Fermi branch are found to be in very good agreement with shell-model predictions in spite of fundamental differences between these models concerning model space, treatment of correlations, or inclusion of a core. This result indirectly supports the two-body-current-based scenarios behind the quenching of the axial-vector coupling constant.

DOI: 10.1103/PhysRevC.93.042501

Atomic nuclei are unique laboratories for the study of fundamental processes and the search for possible signals of *new physics* beyond the standard model in ways that are complementary or even superior to other sciences. Traditionally, they are used to study the weak interaction. A flagship example is the superallowed $I = 0^+ \rightarrow I = 0^+$ β-decay among the members of the isobaric triplets $T = 1$. With small, on the order of 1%, theoretical corrections accounting for radiative processes and isospin symmetry breaking (ISB), these semileptonic pure Fermi (vector) decays allow one to verify the conserved vector current (CVC) hypothesis with a very high precision. In turn, they provide the most precise values of the strength of the weak force, $G_{\rm F}$, and of the leading element, $V_{\rm ud}$, of the Cabbibo-Kobayashi-Maskawa (CKM) matrix, see [1] for a recent review.

The $T = 1/2$ mirror nuclei offer an alternative way to test the CVC hypothesis [2]. These nuclei decay via the mixed Fermi and Gamow-Teller (GT) transitions. Hence, apart from the radiative and the ISB theoretical corrections, the final values of $G_{\rm F}$ and $V_{\rm ud}$ depend on the ratio of statistical rate functions for the axial-vector and vector interactions, $f_{\rm A}/f_{\rm V}$, and the ratio of nuclear matrix elements $\rho \approx \lambda M_{\rm GT}/M_{\rm F}$ where $\lambda = g_{\rm A}/g_{\rm V}$ denotes the ratio of axial-vector and vector coupling constants.

The CVC hypothesis implies that the vector coupling constant is a true constant $g_{\rm V} = 1$. The axial-vector current is partially conserved, meaning that the coupling constant gets renormalized in a nuclear medium. The effective axial-vector coupling constant, $g_A^{\rm (eff)} = q g_{\rm A}$, is quenched by an A-dependent factor, q, with respect to its free neutron decay value $g_{\rm A} \approx -1.2701(25)$. Quenching factors deduced from comparisons between the large-scale nuclear shell-model (NSM) calculations and experiment are $q \approx 0.82$, $q \approx 0.77$ [3], and $q \approx 0.74$ [4] in the p, sd, and pf shells, respectively. In heavier, $A = 100$–134, nuclei, the average quenching is $q \approx 0.48$ [5]. This result is consistent, up to a theoretical uncertainty, with the result of Ref. [6]. Even stronger quenching, $g_{\rm A} A^{-0.18}$, is used in the IBM-2 model [7].

The question about physical causes of the quenching has no unique answer. The quenching is usually related to (i) missing correlations in the wave function, (ii) truncation of model space, or (iii) to a very fashionable nowadays renormalization of the GT operator due to the two-body currents [8,9]. Scenarios involving non-nucleonic degrees of freedom like $NN \rightarrow N\Delta$ excitations are shown to contribute only rather weakly [10].

Proper understanding of quenching is essential for many branches of modern physics from modeling of astrophysical processes in stars to elusive neutrinoless double-β decay. To address quenching, it is of paramount importance to investigate the GT matrix elements (MEs) using diverse theoretical models. The goal of this work is to communicate the pioneering application of the multireference density functional theory (MR-DFT) rooted no-core-configuration-interaction (NCCI) approach to study β decay, with a particular emphasis on the GT process. After a short introduction to the model we shall present the numerical results starting with the β decay of ^{6}He in order to test reliability of the model. Afterward, the model will be applied to the sd- and lower pf-shell $T = 1/2$ mirror nuclei, where both the GT MEs and the Fermi MEs will be computed.

The NCCI models rooted in MR-DFT offer nowadays an interesting alternative to the conventional nuclear shell model [11–13]. First, they are capable of treating rigorously both the fundamental (spherical, particle number) as well as approximate (isospin) symmetries. Second, by invoking the generator coordinate method and/or mixing of discrete (quasi)particle-(quasi)hole (or particle-hole) configurations, they allow one to incorporate important correlations into the nuclear wave function. Third, they can be applied to any nucleus irrespective of A and the neutron and proton number parities. Moreover, by construction, they are able to capture core-polarization effects resulting from a subtle interplay between the long- and short-range nucleon-nucleon forces, which is of critical importance for the calculation of isospin impurities and ISB corrections [14].

The NCCI formalism developed by our group [12,13] involves the angular momentum and isospin projections and subsequent mixing of states having good angular momentum and properly treated isospin. It proceeds in three distinct steps. First, we compute self-consistently a set of k Hartree-Fock (HF) (multi)particle-(multi)hole configurations, $\{|\varphi_j\rangle\}_{j=1}^{k}$,

relevant for the problem under study. The Slater determinants $\{|\varphi_j\rangle\}_{j=1}^{k}$ are calculated using the Hamiltonian consisting of Coulomb and density-independent Skyrme interactions. The use of density-independent *true* Skyrme interaction is a serious limitation but, at present, is the only alternative allowing us to avoid singularities [15,16] at the next stage, at which we apply the angular momentum and isospin projections to determine, for each j, the family of states $\{|\varphi_j; IMK; TT_z\rangle\}$ having good isospin TT_z, angular momentum IM, and angular-momentum projection on the intrinsic axis K. Subsequently, the states $\{|\varphi_j; IMK; TT_z\rangle\}$ are mixed in order to account for the K and isospin mixing. This gives a set of good angular-momentum states $\{|\varphi_j;\ IM; T_z\rangle^{(i)}\}_{i=1}^{I_j}$ with properly treated isospin mixing for each HF configuration j [14,17]. The set is nonorthogonal and, in general, over complete. In the final step, the states are mixed over different configurations by solving the Hill-Wheeler-Griffin (HWG) equation, $\hat{H}u = ENu$, with the same Hamiltonian that was used at the HF level. The HWG equation is solved in the *collective space* spanned by the *natural states* corresponding to nonzero eigenvalues n of their norm matrix N. The same technique is used in the code to handle K mixing alone as described in detail in Ref. [18].

On exit, the NCCI code provides eigenfunctions that are labeled by the index n numbering eigenstates in ascending order according to their energies and the strictly conserved quantum numbers I, M, and $T_z = (N - Z)/2$. The eigenstates can be decomposed in the original projected (nonorthogonal) basis:

$$|n;\ IM;\ T_z\rangle = \sum_{i,j} a_{ij}^{(n;IM;T_z)} |\varphi_j;\ IM; T_z\rangle^{(i)} = \sum_{i,j} \sum_{K,T\geqslant|T_z|} f_{ijKT}^{(n;IM;T_z)} \hat{P}^T_{T_zT_z} \hat{P}^I_{MK} |\varphi_j\rangle, \quad (1)$$

where $\hat{P}^T_{T_zT_z}$ and $\hat{P}^I_{MK}$ stand for the isospin and angular-momentum projection operators, respectively. This form is particularly useful to compute MEs of the GT operator:

$$M_{\mu,\nu} \equiv \mp\langle n';\ I'M';\ T'_z|\mathcal{O}_{\mu,\nu}|n;\ IM;\ T_z\rangle, \quad (2)$$

where $\mathcal{O}_{\mu,\nu} = \frac{1}{\sqrt{2}} \sum_k^A \hat{\tau}^{(k)}_{1\mu} \hat{\sigma}^{(k)}_{1\nu}$ is expressed by means of one-body spherical tensors. The isospin index above is fixed $\mu = \pm 1$ and it determines the overall phase factor. The matrix element (2) fulfills the Wigner-Eckart theorem

$$M_{\mu,\nu} = \frac{1}{\sqrt{2I'+1}} C^{I'M'}_{IM,1\nu} \langle n', I'||\mathcal{O}_\mu||n, I\rangle, \quad (3)$$

where $C^{I'M'}_{IM,1\nu}$ stands for the Clebsch-Gordan coefficient. The reduced matrix element equals

$$\langle n', I'||\mathcal{O}_\mu||n, I\rangle = \mp \sum_{ijKT} \sum_{i'j'K'T'} f^{(n';I'M';T'_z)^*}_{i'j'K'T'} f^{(n;IM;T_z)}_{ijKT} \times \sqrt{2I'+1}\, C^{T'T'_z}_{TT_z,1\mu} \sum_{\eta,\xi} C^{T'T'_z}_{TT'_z-\eta,1\eta} C^{I'K'}_{IK'-\xi,1\xi} J^{(TT_zT'_z;IKK')}_{\eta,\xi;j,j'}. \quad (4)$$

The integral J runs over the β Euler angle in isospace, β_T, and the Euler angles in space $\Omega = (\alpha, \beta, \gamma)$:

$$J^{(TT_zT'_z;IKK')}_{\eta,\xi;j,j'} = \frac{2T+1}{2} \int_0^\pi d\beta_T \sin\beta_T\, d^T_{T'_z-\eta,T_z} \times \frac{2I+1}{8\pi^2} \int d\Omega\, D^{I*}_{K'-\xi,K} \langle\varphi_{j'}|\mathcal{O}_{\eta,\xi}|\tilde{\tilde{\varphi}}_j\rangle, \quad (5)$$

where $d^T_{T'_z,T_z}$ and $D^I_{M,K}$ are the Wigner functions and $\tilde{\tilde{\varphi}}_j$ denotes the Slater determinant rotated in space and isospace. Mean-field (MF) matrix elements in Eq. (5) can be expressed by means of transition densities. The formulas are somewhat lengthy and will be published in our forthcoming paper. All integrals appearing above can be calculated exactly by applying appropriate quadratures, see [18] for further details.

The Wigner-Eckart relation (3) implies that the total probability of decay summed up over the components ν of the operator $\mathcal{O}_{\mu,\nu}$ and over polarizations of the final state M' is

$$B(\mathcal{O}_\mu; n, I \to n', I') = g_A^2 \frac{|\langle n', I'||\mathcal{O}_\mu||n, I\rangle|^2}{2I+1} \equiv g_A^2 \frac{|M_{GT}|^2}{2I+1}. \quad (6)$$

The calculations discussed below were done using a new unpublished version of the HFODD solver [18,19], which was equipped with the NCCI module. To track mean-field (MF) configurations and facilitate convergence properties at the MF level all reference states used in the NCCI calculations were self-consistently calculated assuming parity and signature symmetries. In the calculations we used a basis consisting of either $N = 10$ or 12 spherical harmonic oscillator (HO) shells. The calculations were performed using either the SV Skyrme force of Ref. [20] or a variant of this force, dubbed SV_{SO}, having 20% stronger spin-orbit interaction. The latter force was introduced to improve slightly the single-particle (s.p.) properties of the SV, in particular, by shifting the $d_{3/2}$ subshell with respect to the $s_{1/2}$ subshell. The near degeneracy of these subshells in the SV energy density functional (EDF) causes strong mixing and, in turn, leads to unphysically large ISB corrections in the superallowed $0^+ \to 0^+$ β-decay in $A = 38$ isospin triplet [14]. The SV_{SO} force does not cure the problem of incorrectly placed s.p. levels but makes the spectrum slightly more realistic. Indeed, in ^{40}Ca, the $s_{1/2}$ and $d_{3/2}$ neutron subshells are separated by 0.22 MeV in the SV EDF and 1.18 MeV in the SV_{SO} EDF, respectively. For comparison, the experimental splitting is 2.55 MeV [21].

It should be also mentioned here that the Skyrme interactions are almost ultimately fitted to time-even observables. In turn, their spin-isospin properties are strongly parametrization dependent [22,23], which impairs the calculated charge-changing processes as demonstrated in Ref. [24]. To improve the reliability of the calculated spin-isospin observables the Skyrme forces should be refitted to include carefully selected time-odd data, which is, however, beyond the scope of the present work.

Recently, Knecht *et al.* [25] performed high-precision measurement of the $0^+ \to 1^+$ β decay of ^{6}He, which proceeds exclusively to the ground state (GS) of ^{6}Li and determined

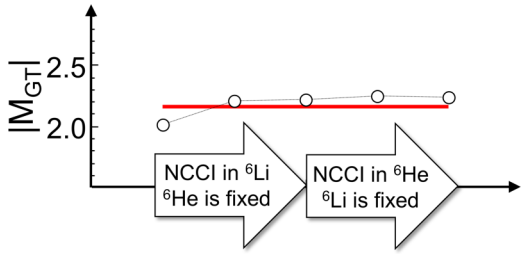

FIG. 1. GT ME for β decay of ^{6}He as a function of a number of configurations taken in the NCCI calculations in ^{6}Li and ^{6}He. Solid line shows the experimental value of Ref. [25].

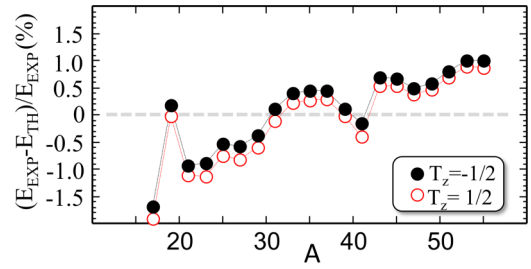

FIG. 2. Theoretical binding energies of $T = 1/2$ mirror nuclei calculated using the NCCI framework. The results are shown relative to the experimental data.

the corresponding GT matrix element $|M_{\rm GT}| = 2.1645(43)$ assuming $g_{\rm A} = -1.2701(25)$. This is an excellent test case for our model mainly because of a limited number of *ph* configurations that can contribute in these *p*-shell nuclei.

The results of the NCCI calculations performed for this transition are depicted in Fig. 1. The figure shows the calculated GT ME versus a number of configurations taken in the mixing. The very left point corresponds to a situation where no mixing was performed in either of the nuclei. In this limit, called hereafter the MR-DFT limit, the HF reference states were selected based ultimately on the energy criterion. Note that already in this limit the calculated ME is in fair agreement with the empirical value underestimating it by ≈7%. Next, keeping the wave function of ^{6}He fixed, we attempted to correlate the wave function of ^{6}Li by admixing 1^+ states projected from the lowest *ph* configuration (second point) and from the first two lowest *ph* configurations (third point). This caused an increase of the ME to 2.208 and 2.223, respectively, i.e., circa 3% above the experiment, see Fig. 1. At this point we froze the wave function of ^{6}Li and attempted to correlate the wave function of ^{6}He (last two points). This weakly influenced the ME giving eventually 2.238.

The test shows that the model is capable of capturing the main features of the wave functions that are important for reliable reproduction of the GT ME and provides stable predictions as a function of a number of admixed configurations. It is worth noticing that an even better result, $|M_{\rm GT}| = 2.185$, can be obtained based on a simple *p*-shell configuration interaction calculation involving the surface-δ interaction, see [26] for further details. These results seem to indicate rather weak sensitivity of this specific decay to the details of underlying nucleon-nucleon interactions. This conjecture will be thoroughly examined below.

Encouraged by the result obtained for the ^{6}He decay, we performed a systematic study of the GT and Fermi MEs for the GS → GS transitions in the $T = 1/2$ mirror nuclei covering the *sd*- and lower *pf*-shell nuclei from $A = 17$ to 55. All results shown below were obtained using the SV$_{\rm SO}$ EDF. This functional, apart from slightly more realistic s.p. levels, is also superior in reproducing binding energies (BEs) in comparison to the SV EDF. The ability to reproduce masses is considered to be one of the most important signatures of the quality of DFT-rooted models. The calculated BEs relative to empirical results are depicted in Fig. 2. Although the theory tends to overbind the lightest species and underbind the heavier, the overall agreement is at a quite impressive level of ±1%. It is better almost by a factor of 2 than the level of agreement obtained for the SV interaction.

It appears also that the SV$_{\rm SO}$ has reasonable spectroscopic properties. The theory is able to reproduce the GS spins already at the MR-DFT level with the exception of the $A = 19$ case, where the model predicts $I = 5/2^+$ instead of $I = 1/2^+$ to be the GS spin. The energy spectra are, in general, in fair agreement with the data. For the sake of illustration, Fig. 3 shows theoretical and experimental $I = 3/2^+$ and $5/2^+$ states in the lower *sd*-shell nuclei. Similar agreement is obtained for heavier nuclei.

Figure 4 shows the GT MEs, $|g_{\rm A} M_{\rm GT}|$, calculated using the MR-DFT and the NCCI models. The NCCI calculations involve typically four to five low-lying *ph* MF configurations. The results of both approaches are strikingly similar except for the ^{45}V → ^{45}Ti transition. Both models systematically overestimate the data beside the nuclei ranging from $A = 29$ to 35. Strong suppression of the GT MEs in this mass range is related to the aforementioned clustering of the $s_{1/2}$ and $d_{3/2}$ subshells in MF calculations. Proximity of these two subshells causes strong mixing, which has a destructive impact on the calculated MEs. Comparison of the MR-DFT results obtained using the SV and SV$_{\rm SO}$ EDFs supports this conclusion. Indeed, the MEs calculated using these two functionals are almost identical everywhere except for the mass region discussed above.

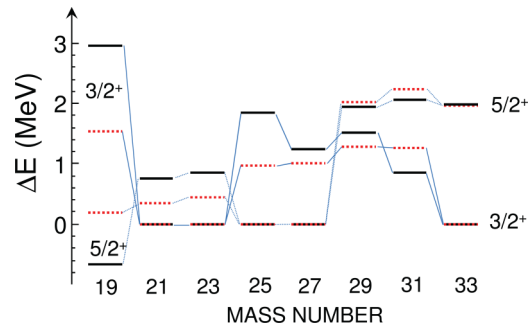

FIG. 3. Excitation energies of the lowest $3/2^+$ and $5/2^+$ states in *sd*-shell $T = 1/2$, $T_z = 1/2$ nuclei ranging from $A = 19$ to 33. The calculated (experimental) levels are marked by thick solid (dashed) lines. The calculated states come from MR-DFT. Theoretical energies have been normalized to the experimental ground states.

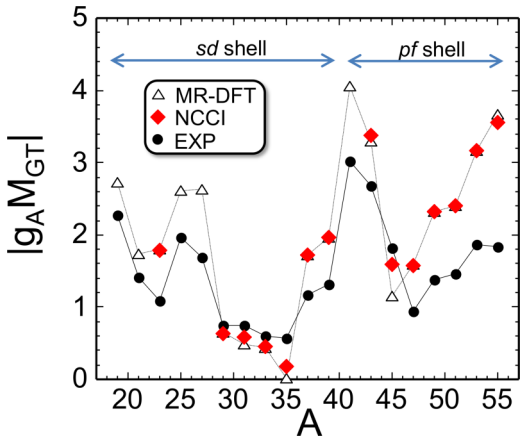

FIG. 4. Gamow-Teller matrix elements calculated using the MR-DFT (triangles) and NCCI (diamonds) approaches in comparison with experimental data (dots) taken from Ref. [3] (*sd* shell) and Refs. [4,27] (*pf* shell).

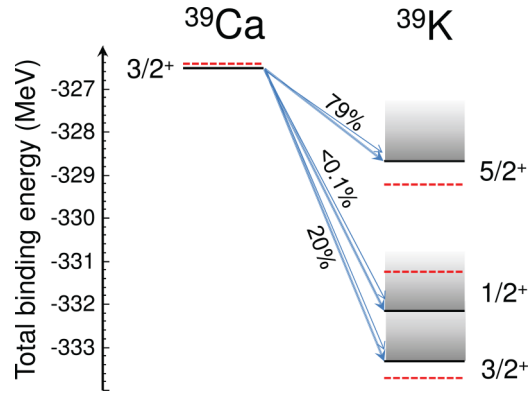

FIG. 6. Ikeda sum rule for the GS of ^{39}Ca. Thick horizontal lines indicate the theoretical (solid) and experimental (dashed) total BEs of the GS in ^{39}Ca and the lowest $1/2^+$, $3/2^+$, and $5/2^+$ states in ^{39}K. The numbers over the arrows indicate the total calculated GT strength for each I. Multiple arrows and shadowing indicate that the strength is distributed over several states.

Figure 5 shows the NCCI results in comparison to the NSM calculations of Ref. [3] (*sd* shell) and Refs. [4,27] (*pf* shell). The two sets of calculations are very consistent with each other. Indeed, a linear fit to the MR-DFT (NCCI) GT MEs gives $q = 0.77$ (0.78) in the *sd* shell (excluding problematic $A = 31$–35 cases) and $q = 0.75$ (0.69) in the lower *pf* shell, respectively. These values agree almost perfectly with the NSM quenching in spite of numerous differences between the models. In particular, our model (i) includes the core and takes into account core polarization effects, (ii) accounts for correlations in a different, more schematic way, than the shell-model, (iii) uses functionals, which were not optimized for the NCCI calculations, or (iv) uses completely different model space. To address the last point, we performed an additional set of MR-DFT calculations using a larger basis, consisting of $N = 12$ spherical HO shells. We found that the increase of the basis size has almost no impact on the calculated MEs. Note also, a systematic difference between

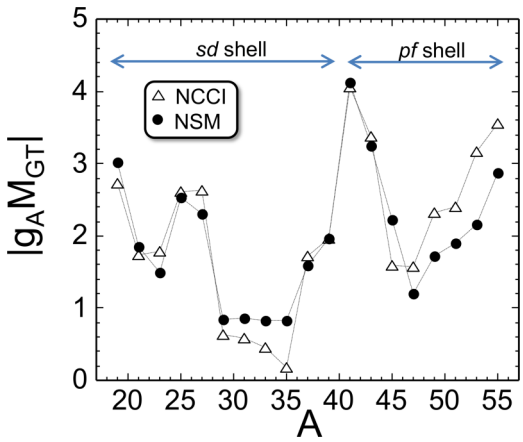

FIG. 5. GT MEs calculated using the NCCI model (triangles) in comparison to the NSM results of Ref. [3] (*sd* shell) and Refs. [4,27] (*pf* shell).

the shell-model and NCCI results in the heaviest calculated nuclei. The origin of this difference requires deeper study.

The Ikeda sum rule is an important indicator of the quality of theoretical models. For the $T = 1/2$ mirrors it takes a particularly simple form: $\sum_{n',I'} B(\mathcal{O}_+; n, I \to n', I') = 3$. Systematic study of the Ikeda sum rule with the present formalism involving the isospin and angular momentum projections is CPU expensive. Hence, it was limited here to one of the simplest cases of $A = 39$ nuclei. In this case, inclusion of all possible *ph* excitations within the *sd* shell exhausts 99% of the sum rule as illustrated in Fig. 6. It is worth mentioning that inclusion of *ph* excitations between the spin-orbit partners $d_{5/2} \to d_{3/2}$ is crucial for the sum rule. More systematic study of the sum rules will be done with the variant involving only the angular-momentum projection.

The use of the NCCI approach involving both the isospin and angular-momentum projected states is absolutely necessary to study Fermi transitions and, in particular, to extract the ISB corrections to the Fermi branch of β decay. Let us recall that the ISB corrections are needed to study the CVC hypothesis and the CKM matrix via the transitions in the mirrors, see Ref. [2]. The results obtained in this study are collected in Table I. It is beneficial to see that our corrections are very consistent with the NSM results of Ref. [28].

In summary, we have presented a systematic study of the GS $\to$ GS GT and Fermi MEs in $T = 1/2$ mirror nuclei using, for the first time, the NCCI approach based on the isospin and angular-momentum projected MR-DFT formalism. The framework is universal and can be applied to any nucleus irrespective on its mass and the proton and neutron number parities. It can be also improved and optimized in many different ways, in particular, concerning the tensor force which is known to have an impact on the shell structure [29,30] and β decay [31].

In the present implementation with the SV or SV_{SO} EDFs the calculated GT MEs systematically overestimate experimental data for the free neutron strength of the axial current. The level of disagreement is found to be very similar

TABLE I. Theoretical ISB corrections $\delta_C^{(NCCI)}$ (in %) adopted in this work. For the sake of comparison the table contains also the NSM results, $\delta_C^{(NSM)}$, of Ref. [28].

A	$\delta_C^{(NCCI)}$	$\delta_C^{(NSM)}$	A	$\delta_C^{(NCCI)}$	$\delta_C^{(NSM)}$
17	0.166(17)	0.585(27)	37	0.907(91)	0.734(61)
19	0.339(34)	0.415(39)	39	0.318(32)	0.855(81)
21	0.300(30)	0.348(27)	41	0.426(43)	0.821(63)
23	0.316(32)	0.293(22)	43	0.690(69)	0.50(10)
25	0.413(41)	0.461(47)	45	0.589(59)	0.87(12)
27	0.439(44)	0.312(34)	47	0.673(67)	
29	0.520(52)	0.976(53)	49	0.646(65)	
31	0.585(59)	0.715(36)	51	0.714(71)	
33	0.705(71)	0.865(59)	53	0.898(90)	
35	0.366(37)	0.493(46)	55	0.620(62)	

to the one obtained using a large-scale shell model in spite of the fundamental differences between the two approaches in handling the core and the core polarization effects, the correlations, or the basis truncation. It strongly suggests that the mechanism of in-medium renormalization of the axial strength may indeed be related to the two-body currents. This conjecture requires further study. It is, however, very appealing because the two-body currents do not renormalize the Fermi transition operator [8] in agreement with the experimental data and theoretical results on superallowed $0^+ \rightarrow 0^+$ Fermi decays [1,14].

Finally, we also calculated the ISB corrections to the Fermi decay branch in the $T = 1/2$ mirror nuclei. The corrections turned out to be in very good agreement with the NSM calculations.

This work was supported in part by the Polish National Science Centre (NCN) under Contracts 2012/07/B/ST2/03907 and 2014/15/N/ST2/03454. The CSC-IT Center for Science Ltd., Finland, is acknowledged for the allocation of computational resources.

[1] J. C. Hardy and I. S. Towner, J. Phys. G: Nucl. Part. Phys. **41**, 114004 (2014).
[2] O. Naviliat-Cuncic and N. Severijns, Phys. Rev. Lett. **102**, 142302 (2009).
[3] B. A. Brown and B. H. Wildenthal, At. Data Nucl. Data Tables **33**, 347 (1985).
[4] G. Martínez-Pinedo, A. Poves, E. Caurier, and A. P. Zuker, Phys. Rev. C **53**, R2602 (1996).
[5] P. Pirinen and J. Suhonen, Phys. Rev. C **91**, 054309 (2015).
[6] E. Caurier, F. Nowacki, and A. Poves, Phys. Lett. B **711**, 62 (2012).
[7] J. Barea, J. Kotila, and F. Iachello, Phys. Rev. C **91**, 034304 (2015).
[8] J. Menéndez, D. Gazit, and A. Schwenk, Phys. Rev. Lett. **107**, 062501 (2011).
[9] A. Ekström, G. R. Jansen, K. A. Wendt, G. Hagen, T. Papenbrock, S. Bacca, B. Carlsson, and D. Gazit, Phys. Rev. Lett. **113**, 262504 (2014).
[10] M. Ichimura, H. Sakai, and T. Wakasa, Prog. Part. Nucl. Phys. **56**, 446 (2006).
[11] B. Bally, B. Avez, M. Bender, and P.-H. Heenen, Phys. Rev. Lett. **113**, 162501 (2014).
[12] W. Satuła, J. Dobaczewski, M. Konieczka, and W. Nazarewicz, Acta Phys. Polonica B **45**, 167 (2014).
[13] W. Satuła, J. Dobaczewski, and M. Konieczka, JPS Conf. Proc. **6**, 020015 (2015).
[14] W. Satuła, J. Dobaczewski, W. Nazarewicz, and M. Rafalski, Phys. Rev. Lett. **106**, 132502 (2011).
[15] M. Anguiano, J. L. Egido, and L. M. Robledo, Nucl. Phys. A **696**, 467 (2001).
[16] D. Lacroix, T. Duguet, and M. Bender, Phys. Rev. C **79**, 044318 (2009).
[17] W. Satuła, J. Dobaczewski, W. Nazarewicz, and M. Rafalski, Phys. Rev. Lett. **103**, 012502 (2009).
[18] J. Dobaczewski *et al.*, Comput. Phys. Commun. **180**, 2361 (2009).
[19] N. Schunck, J. Dobaczewski, J. McDonnell, W. Satuła, J. A. Sheikh, A. Staszczak, M. M. Stoitsov, and P. Toivanen, Comput. Phys. Commun. **183**, 166 (2012).
[20] M. Beiner, H. Flocard, N. V. Giai, and P. Quentin, Nucl. Phys. A **238**, 29 (1975).
[21] A. Oros, Ph.D. thesis, University of Köln, 1996.
[22] M. Bender, J. Dobaczewski, J. Engel, and W. Nazarewicz, Phys. Rev. C **65**, 054322 (2002).
[23] H. Zduńczuk, W. Satuła, and R. A. Wyss, Phys. Rev. C **71**, 024305 (2005).
[24] W. Almosly, B. G. Carlsson, J. Dobaczewski, J. Suhonen, J. Toivanen, P. Vesely, and E. Ydrefors, Phys. Rev. C **89**, 024308 (2014).
[25] A. Knecht *et al.*, Phys. Rev. Lett. **108**, 122502 (2012).
[26] J. Suhonen, *From Nucleons to Nucleus: Concepts of Microscopic Nuclear Theory* (Springer, Berlin, 2007).
[27] T. Sekine, J. Cerny, R. Kirchner, O. Klepper, V. T. Koslowsky, A. Plochocki, E. Roeckl, D. Schardt, and B. Sherrill, Nucl. Phys. A **467**, 93 (1987).
[28] N. Severijns, M. Tandecki, T. Phalet, and I. S. Towner, Phys. Rev. C **78**, 055501 (2008).
[29] T. Otsuka, R. Fujimoto, Y. Utsuno, B. A. Brown, M. Honma, and T. Mizusaki, Phys. Rev. Lett. **87**, 082502 (2001).
[30] M. Zalewski, J. Dobaczewski, W. Satuła, and T. R. Werner, Phys. Rev. C **77**, 024316 (2008).
[31] F. Minato and C. L. Bai, Phys. Rev. Lett. **110**, 122501 (2013).